Journal of the Taiwan Institute of Chemical Engineers 121 (2021) 229–240

Contents lists available at ScienceDirect

Journal of the Taiwan Institute of Chemical Engineers

journal homepage: www.elsevier.com/locate/jtice

Investigation on the improvement of the combustion process through hybrid dewatering and air pre-heating process: A case study for a 150 MW coal-fired boiler

Oguz Arslan[a,*], Oguzhan Erbas[b]

[a] Thermodynamics Division, Mechanical Engineering Department, Engineering Faculty, Bilecik Seyh Edebali University, Bilecik 11000, Turkey
[b] Energy Division, Mechanical Engineering Department, Engineering Faculty, Kutahya Dumlupinar University, Kutahya 43100, Turkey

ARTICLE INFO

Article History:
Received 16 December 2020
Revised 18 March 2021
Accepted 10 April 2021
Available online 21 April 2021

Keywords:
Advanced exergy
Air preheating
Coal-fired boiler
Combustion
Dewatering
Waste heat

ABSTRACT

In this study, a parametric advanced exergy analysis was conducted for the waste heat recovery of a pulverized coal-fired power plant. In this aim, a new attainable ideal and the technically available unavoidable case for the combustion process were identified. Under the identified improved potential term, different unavoidable cases were parametrically investigated for the hybrid dewatering and air preheating process to improve the combustion process. In this aim, different removed moisture contents, air preheating conditions, and effectiveness of both internal and external heat exchangers were thermodynamically evaluated in terms of the combustion process. The improved potential was calculated as 74.4% for the whole combustion system. The critical moisture removal ratio was calculated as 20%. The effects of rehabilitation on improved potential were found as 2.80 points per 1% of effectiveness increase for the self (internal) heat exchangers of the boiler, 1.68 points per 1% of effectiveness increase for HE-I and HE-II (external heat exchangers), and 0.62 points per 1% increase of dewatered moisture ratio. Besides, a saving of about 29.54% was determined in fuel consumption for the most appropriate unavoidable condition.

1. Introduction

Depending on the large reservoirs, lignite is an indispensable source to meet the thermal and electrical energy demand for Turkey. By the end of the first half of 2019, 22.4 percent of electricity generation was provided from coal-fired power plants [1]. Due to their low efficiencies, these technologies need to be developed or to be improved on a component basis at least. The studies conducted on the coal-fired power plants show that the most exergy destructive component is the boiler system depending on the nature of the combustion process. In Table 1, a brief summary of the literature review on the exergy destruction values of the boiler system for the coal-fired power plants is given.

According to Table 1, the exergy destruction rates of the boiler could reach up to 91% of the total exergy destruction of the overall power plant. Therefore, the boilers are the most important components that should be early taken into consideration. The leading recuperations, which improve the combustion process without any changes of the boiler's self-components, can be sorted as the air preheating and dewatering processes. In the literature, there are many studies conducted on boiler recuperation. A brief summary of the literature review is given in Table 2.

The preheating of the combustion air by the flue gases is the most common application to improve combustion efficiency. This method enables the improvement of the combustion efficiency of the boiler along with the recovery of the waste heat of the flue gases. It was reported that saving about 10% of heater fuel is possible by the increase of 200 °C in the combustion air temperature [27]. It was also reported that it is possible to increase the combustion efficiency up to 99.72% by the process of air preheating [13]. It is available to increase the energy efficiency of the plant by 0.64% [14] and the exergetic efficiency of the plant by 0.48% [15]. Also, it is available to reduce the fuel consumption in an amount of 5.38 g per hourly-generated electricity that means a reduction of the discharged pollutant by about 1.48% [16].

The other common application is to remove the moisture content for the increase of coal quality. It was reported that 20–25% of the combustion energy was wasted for the removal of water content in the combustion process [28]. In this regard, the dewatering process, of course, would make a positive effect. The dewatering process has also a secondary advantage preventing the ignition delay by the preheating of the fuel. This indirect effect of the dewatering process

Abbreviations: B, boiler; CC, combustion chamber; CS, combustion system; *DMR*, dewatered moisture ratio; G, generator; HE-I, air preheater; HE-II, drying air heater; R, reheater; SH, superheater

* Corresponding author.
E-mail address: oguz.arslan@bilecik.edu.tr (O. Arslan).

https://doi.org/10.1016/j.jtice.2021.04.012
1876-1070/

Nomenclature

$\dot{E}$	energy rate (kW)
$\dot{E}x$	exergy rate (kW)
h	specific enthalpy (kJ/kg)
$\overline{h}$	specific molar enthalpy (kJ/kmole)
I	exergy destruction rate (kW)
IP	improvement potential (%)
IP^*	improved potential (%)
$\dot{m}$	Mass flow rate (kg/s)
$\dot{n}$	molar rate (kmole/s)
P	Pressure (kPa, bar, or atm)
$\dot{Q}$	heat rate (kW)
R_u	universal gas constant (kJ/kmole K)
s	specific entropy (kW/kg K)
T	temperature (K or °C)
$\dot{W}$	work rate (kW)
x	molar fraction

Greek symbols

ε	exergy efficiency (%)
η	effectiveness (%)
λ	coefficient of excess air
ϕ	relative moisture content (%)
ψ	specific flow exergy (kJ/kg)

Subscripts

cc	combustion chamber
d	destruction
f	fuel
g	generated
i	inlet or ith component
k	kth component
o	outlet
p	product or reactant
T	value at a specified temperature
0	value at the reference state

Superscripts

f	formation
Q	exergy term related to heat
W	exergy term related to work
o	absolute
EX	exogenous
EN	endogenous
AV	avoidable
UN	unavoidable

results in saving of the fuel consumption and decrease of the emission [29,30]. It is possible to obtain an efficiency increase in the power unit by about 1.0–2.5% by the dewatering process [31]. The steam pre-drying, flue gas pre-drying, and air pre-drying systems are commonly used in coal-fired power plants for the recovery of waste heat. An increase in the plant efficiency was recorded as 2.19% for the steam dryer where it was 1.55% for the flue gas dryer [21]. Rao et al. [32] indicated that the use of waste heat from the boiler exhaust gases is the best way for a drying and dewatering system near a power plant since the location where drying technologies are employed is an important factor. From this point, the flue gas drying systems come into prominence for the recovery of waste heat after the air preheater in the coal-fired power plants.

The better way to improve efficiency is to use the coupled air preheating and dewatering processes. Han et al. [33] used the hot flue gases taken after the superheater for the drying process. The dryer exhaust was used for the pre-heating of the combustion air. Finally, the exhaust of the boiler was used to heat the pre-heated air in the main air heater. They reported an efficiency increase of 1.51% in the plant efficiency. Han et al. [34], in a different study, used the hot flue gases taken before the superheater. They used the exhaust of the dryer for the preheating purpose of the combustion air. They reported an efficiency increase of 1.70% in the plant efficiency. Han et al. [35] reported an increase of 3.42% in the plant efficiency was available by the coupled air preheating and dewatering processes. This recuperation also provided an advantage of a decrease of 2.32% in the exergy destruction of the combustion process. Although the systems in which the flue gas is used directly as the moisture removal media have more efficient drying, Nikolopoulos et al. [36] indicated that the low-temperature air-dryers have recently received significant interest for the drying systems because of the low-grade heat source. Therefore, a low-temperature air-dryer sourced by flue gases is used in this study. Also, the drying air is heated by the flue gases taken after the air heater to protect the main structure of the boiler.

In this study, the concurrent effect of the pre-heated air and dewatered coal was thermodynamically investigated concerning the improvement of the combustion process of a 150 MW coal-fired boiler. Advanced exergy analysis was conducted for this aim since it enables to observe the irreversibilities sourced by internal and external factors for an existing state of any system. In the analysis, the conditions of steam at the outlet of the boiler were kept constant to discriminate the exogenous effects of the other components of the plant on the boiler. Besides, the operating conditions of the boiler self-components (except for air pre-heater) such as superheater, re-heater, and economizer were also kept constant. A conceptual design was formed combining the air-preheater and air pre-dryer to observe the concurrent effects of pre-heated air and dewatered lignite. The air pre-heater system also was analysed separately to observe the single effect of pre-heated air. Six different unavoidable cases were investigated in this aim.

2. Material and method

Although the advanced exergy analysis is conducted for a whole system with multi-component, it is available to be used for a single component that includes one or more subcomponents [37]. Moreover, it is a useful tool to observe the improvements of the handled component combined with the new systems or new components since it allows to determine the endogenous and exogenous losses keeping the inlet or outlet conditions constant. In this study, the boiler of a coal-fired power plant with a 150 MW installed capacity was taken into consideration. The current boiler system mainly forms of four components namely superheater (SH), re-heater (R), combustion chamber (CC), and economizer (E). Additionally, it includes an air preheater system with lower effectiveness of about 49%. The system is fed by pulverized lignite in a slurry form depending on its moisture content. This moisture content reduces the boiler efficiency affecting the combustion process. A dryer unit can be added to the boiler system using the waste heat of flue gas. Since this addition would affect the air preheating process alongside the combustion, all the processes should concurrently be evaluated. In this regard, a conceptual design was formed to observe the concurrent and separate effects of air preheating and dewatering processes. The schematic of the conceptual design is given in Fig. 1.

According to the conceptual design, the main structure of the boiler was protected. A new heat exchanger (HE-I) was added to the boiler for the air preheating. Besides, another exchanger (HE-II) was also added to the boiler for the dewatering process of the lignite in the dryer. Alternatively, HE-II was coupled with an electrical heater (EH) with an efficiency of 99% for the case in which the waste flue gas was insufficient for the dewatering process of lignite. HE-II is directly connected to an air dryer unit. The power capacity of the electrical heater was determined according to the drying behaviour of the

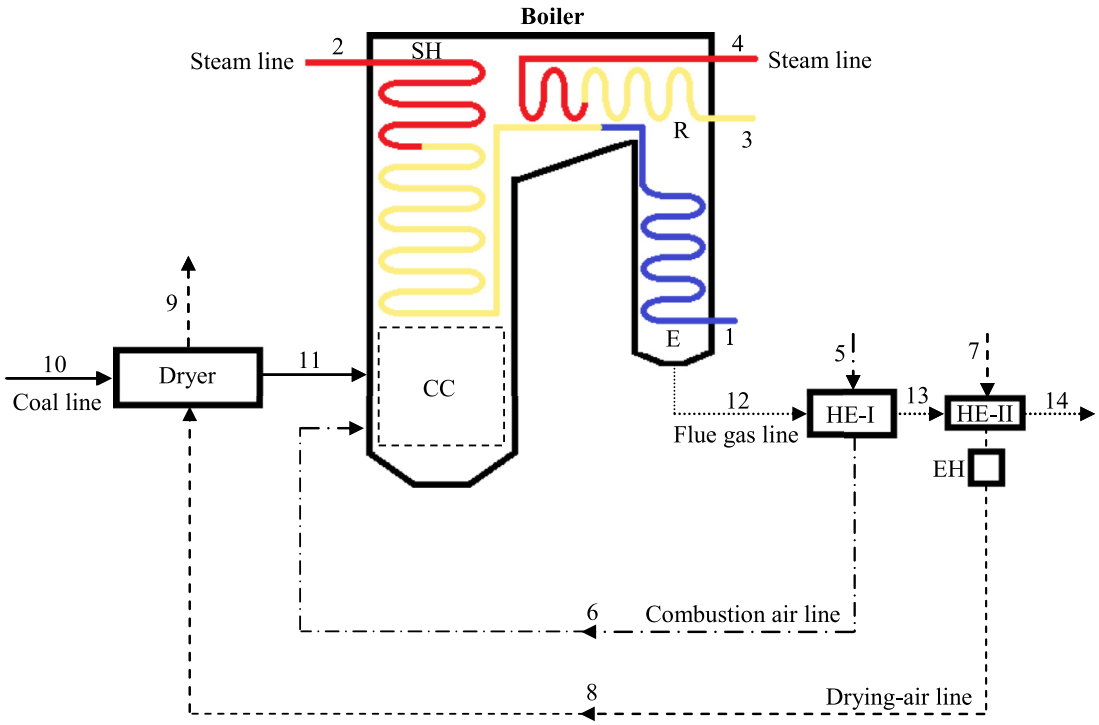

Fig. 1. Flowchart of the conceptual design for dewatering and air preheating.

lignite given by Ref. [38]. The relative moisture content of the air inlet was included as 100% considering the worst case. Taking the low-rank coal into account, the required times for the drying process was determined as 135, 225, and 330 s for the 20, 40, and 60% moisture losses, respectively. The outlet condition of the fresh air was set to 100 °C according to the unavoidable conditions. The required power for the pressure drops of the combustion air line and drying aerial line was supplied by the fans with an efficiency of 90%.

2.1. Combustion analysis

The handled boiler is fed by Seyitomer with relatively higher moisture and ash content about 31.5% and 47.3% by weight in order. The ultimate analysis results of Seyitomer lignite and given in Table 3 [39].

Assuming air is composed of 21.1% of O_2 and 78.9% of N_2, the reaction in CC is given as:

$$\overbrace{(a\cdot C + b\cdot H + c\cdot N + d\cdot S + e\cdot O + f\cdot H_2O_{(fluid)})}^{Fuel} + \lambda\cdot x\cdot \overbrace{(3.76\cdot N_2 + O_2)}^{Air} \rightarrow \overbrace{g\cdot CO + h\cdot CO_2 + j\cdot NO_2 + m\cdot SO_2 + n\cdot O_2 + t\cdot N_2 + v\cdot H_2O_{(gaseous)}}^{Products} \quad (1)$$

Here, λ indicates the coefficient of excess air. In the current combustion case, λ is a relatively higher value with 1.68 (68% excess air). The flue gas compounds were determined by the measured values. The unmeasured values were determined through Eq. (1) taking into account the mass balance. The technical characteristics of measurement equipment and coefficients of combustion reaction are given in Table 4 and Table 5, respectively.

2.2. Energy, exergy and advanced exergy analysis

For the steady-state conditions, neglecting kinetic and potential energy terms, the mass and energy balances for a component of the system are given as;

$$\sum \dot{m}_i - \sum \dot{m}_o = 0 \quad (2)$$

$$\dot{Q} - \dot{W} + \sum \dot{m}_i h_i - \sum \dot{m}_o h_o = 0 \quad (3)$$

where $\dot{Q}$ is heat rate term, $\dot{W}$is work term, $\dot{m}$ is the mass rate. i indicates the inlet conditions and o indicates the outlet conditions. For the combustion process, the energy balance of the boiler is given as:

$$\dot{Q}_f = \sum_i \dot{n}\left(\overline{h}_0^f - \overline{h}_T - \overline{h}_{298}\right) - \sum_o \dot{n}\left(\overline{h}_o^f - \overline{h}_T - \overline{h}_{298}\right) \quad (4)$$

Table 1
A brief summary of the literature of the boiler exergy destruction values for coal-fired power plants.

Author(s)	Explanation	Exergy destruction rate of the boiler	Exergy efficiency of the boiler
Gao et al. [2]	330 MW coal-fired combined heat and power (CHP) plant is investigated.	87.1%	44.10%
Adibhatla and Kaushik [3]	660 MW supercritical coal-fired power plant is investigated.	~90.0%	40.23%
Yang et al. [4]	660 MW ultra-supercritical coal-fired power plant is investigated.	63.9%	67.50%
Hong et al. [5]	600 MW supercritical coal-fired power plant is investigated.	86.3%	–
Regulagadda et al. [6]	32MW coal-fired power plant is investigated.	86.8%	–
Oktay [7]	160 MW fluidized bed coal-fired power plant is investigated.	81.2%	65.00%
Arslan and Acar [8]	150 MW coal-fired power plant is investigated.	70.0%	56.14%
Chauhan and Khanam [9]	250 MW coal-fired power plant is investigated.	89.0%	57.33%
Li and Liu [10]	250 MW coal-fired power plant is investigated.	71.9%	49.69%
Rocha and Silva [11]	660 MW ultra-supercritical coal-fired power plant is investigated.	90.8%	50.67%
Shi et al. [12]	160 MW fluidized bed coal-fired power plant is investigated.	~75.0%	~65.0%

Table 2
A brief summary of the literature review of the recuperation for the boiler.

Author(s)	Explanation	Process	Benefit
Song et al. [13]	A new self-sustained preheating technology for the combustion of the pulverized coal is investigated.	Air preheating	Combustion efficiency up to 99.72%.
Chen et al. [14]	A new air-preheating concept including the integration of a bypass flue-waste heat recovery system is investigated.	Air preheating	Increase of 0.64% in the overall system efficiency. Decrease of 0.94 g/kWh in the fuel consumption.
Chen et al. [15]	A new conceptual design of air preheating system in a 1000 MW coal-fired power plant is investigated.	Air preheating	Increase of 0.48% in the exergetic efficiency of the plant.
Yan et al. [16]	A new method for the recovery of the waste heat of the flue gas is investigated.	Air preheating	Decrease of 5.38 g/kWh in the fuel consumption.
Ma et al. [17]	A novel air preheating system using exhaust gas recirculation is investigated.	Air preheating	Decrease of 3.49 g/kWh in the fuel consumption.
Liu et al. [18]	Thermodynamic analysis of coal-fired plant with steam pre-dryer is conducted	Dewatering	Increase of 1.89% in the plant efficiency.
Ge et al. [19]	The effect of the coal upgraded by dewatering on the combustion process is investigated.	Dewatering	The decrease in activation energy during the combustion stage indicates an important advantage of the utilization of upgraded coals.
Wang [20]	A fluidized bed coal drying system is experimentally investigated	Dewatering	Decrease of 3.8% in auxiliary power consumption by reducing the moisture content from 40% to 25%.
Liu et al. [21]	Thermodynamic analysis of two pre-drying methods namely boiler flue gas drying and steam drying is conducted	Dewatering	Increase of 2.19% and 1.55% in the plant efficiency for steam and flue gas dryer, respectively.
Kakaras et al. [22]	External dryer using flue gases for the fluidized coal-fired power plant is investigated	Dewatering	Increase of 5% in the plant efficiency.
Agraniotis et al. [23]	A pre-dried lignite-fired power system integrated with boiler flue gas drying is investigated.	Dewatering	Increase of 1.5% in the plant efficiency for the case of the firing of 25% pre-dried lignite.
Liu et al. [24]	The incorporation of a rotary-tube steam dryer in a lignite-fired system plant is investigated.	Dewatering	Increase up to 1.90% in plant efficiency.
Xu et al. [25]	A novel concept of steam pre-drying of lignite in a supercritical power plant is investigated.	Dewatering	Increase up to 1.80% in plant efficiency.
Atsonios et al. [26]	Different drying methods for lignite are thermodynamically investigated.	Dewatering	Most effective drying is found as the air dryer using hot water from the feed-water tank. Increase of 0.89% in the plant efficiency.

Here, $\dot{Q}_f$ describes the heat of fuel. $\dot{n}$, $\overline{h}_0^f$, $\overline{h}_T$ and $\overline{h}_{298}$ are respectively the mole ratio, enthalpy of formation, enthalpy at the temperature T, and enthalpy at 298 K. The exergy balances for the k^{th} component of the system, exergy efficiency, and exergy destruction ratios are respectively given as:

$$\dot{E}x_k^Q - \dot{E}x_k^W - \sum(\dot{m}_i\psi_i)_k - \sum(\dot{m}_o\psi_o)_k - \dot{E}x_{d,k} = 0 \tag{5}$$

$$\varepsilon = 1 - \frac{\dot{E}x_{d,k}}{\dot{E}x_{i,k}} \tag{6}$$

$$y_k = \frac{\dot{E}x_{d,k}}{\dot{E}x_{i,k}} \tag{7}$$

$$y_k^* = \frac{\dot{E}x_{d,k}}{\dot{E}x_{d,tot}} \tag{8}$$

where $\dot{E}x_{d,k}$, $\dot{E}x_{i,k}$ and $\dot{E}x_{d,tot}$ describe the exergy destruction rate of the kth component, the exergy inlet to the k^{th} component, and the total exergy destruction rate. $\dot{E}x_k^Q$, $\dot{E}x_k^W$ and ψ respectively describe the exergy of heat, the exergy of the work and the specific exergy of flow, and are given as:

Table 3
Ultimate analysis of the Seyitomer lignite [39].

Compound	weight (%)
C	13.657
S	0.544
N	0.034
O	4.067
H	2.860
Moisture	31.498
Ash	47.340

$$\dot{E}x_k^Q = \left(1 - \frac{T_0}{T}\right)Q_k \tag{9}$$

$$\dot{E}x_k^W = \dot{W}_k \tag{10}$$

$$\psi = (h - h_0) - T_0(s - s_0) \tag{11}$$

$$\psi = c_p\left(T - T_0 - T_0 \cdot ln\left(\frac{T}{T_0}\right)\right) \tag{12}$$

Here, h and s indicate orderly the enthalpy and entropy at a certain state. c_p is the specific heat of gas-phase flow. Subscript of *0* indicates the reference state conditions which are taken as 25 °C and 1 atm in this study. For the combustion process exergy balance of the boiler can be given as [41,42]:

$$\dot{E}x_f = \left(1 - \frac{T_0}{T_{cc}}\right) - I \tag{13}$$

where subscript *cc* indicates the combustion chamber, I describes the exergy destruction rate and is given as [43]:

$$I = \dot{E}x_{d,f} = T_0 S_g \tag{14}$$

$$S_g = S_o - S_i + \frac{\dot{Q}_f}{T_{cc}} \tag{15}$$

where S_o, S_i and S_g are respectively the entropies of products, the entropy of reactants, and generated entropy of fuel-air mixture, and are given by the following equation:

$$S_k = \sum_o \dot{n}_k(\bar{s}_k^o(T, P_0) - R_u ln(x_k P)) \tag{16}$$

Here, $\bar{s}_i^o$, R_u , x_k and P are orderly absolute molar entropy of the kth component, universal gas constant, mole ratio of the kth compound, and total pressure of the flow. The energy and exergy balance

Table 4
Technical data for measurement equipment [40].

Property	IR Thermometer	Digital Thermometer	Gas analyser
Measurement range	−30 / 900 °C	−50/1000 °C	O_2 0–21% CO 100,000 ppm maximum NO_x 4000 ppm maximum SO_2 4000 ppm maximum T_{max} 1000 °C
Sensitivity	± 2 °C (−30. . .−5 °C) ± 0.75 °C (−4.9. . .74.9 °C) ± 0.75% mv (75. . .900 °C)	± 0.7 °C (−50. . .900 °C) ± 1 °C (900.1. . .1000 °C)	O_2 ± 2% CO ± 5% NO_x ± 5% SO_2 ± 5% Temperature ± 2 °C
Solution	0.1 °C	0.1 °C (−50. . .199.9 °C) 1 °C (200. . .1000 °C)	0.1 °C 1 (for emission measurement)

Table 5
Coefficients of combustion balance for ash-free lignite for the real case.

Lignite			Flue gas		
Compound	n (kmole)		Compound	n (kmole)	
C	a	0.0113810	CO_2	g	0.0108745
S	b	0.0001701	CO	h	0.0005065
N	c	0.0000120	SO_2	j	0.0001701
O	d	0.0012708	NO_2	m	0.0000240
H	e	0.0142992	N_2	n	0.1102411
Moisture	f	0.0174991	O_2	t	0.0121200
	x	0.0174540	$H_2O_{(gaseous)}$	v	0.0317983

equations for each system component and the whole system are as given in Table 6.

The exergy destruction for the kth component can be given in the terms of endogenous and exogenous destructions as follows [44]:

$$\dot{E}x_{d,k} = \dot{E}x^{EN}_{d,k} + \dot{E}x^{EX}_{d,k} \tag{17}$$

Endogenous term ($\dot{E}x^{EN}_{d,k}$) is the destruction that occurred within the component sources by the irreversibilities where the exogenous one occurs because of the irreversibilities of working conditions of the other components. Depending on the technological developments, environmental conditions and working parameters, some parts of exergy destructions can be avoided. This part of the destruction is named avoidable exergy destruction ($\dot{E}x^{AV}_{d,k}$). Therefore, the exergy destruction can be given in the terms of avoidable ($\dot{E}x^{AV}_{d,k}$) and unavoidable ($\dot{E}x^{UN}_{d,k}$) destructions as follows [45]:

$$\dot{E}x_{d,k} = \dot{E}x^{AV}_{d,k} + \dot{E}x^{UN}_{d,k} \tag{18}$$

Splitting the endogenous and exogenous parts into avoidable and unavoidable ones, the following equations are observed [46]:

$$\dot{E}x^{EN}_{d,k} = \dot{E}x^{EN,AV}_{d,k} + \dot{E}x^{EN,UN}_{d,k} \tag{19}$$

$$\dot{E}x^{EX}_{d,k} = \dot{E}x^{EX,AV}_{d,k} + \dot{E}x^{EX,UN}_{d,k} \tag{20}$$

$$\dot{E}x^{AV}_{d,k} = \dot{E}x^{EN,AV}_{d,k} + \dot{E}x^{EX,AV}_{d,k} \tag{21}$$

$$\dot{E}x^{UN}_{d,k} = \dot{E}x^{EN,UN}_{d,k} + \dot{E}x^{EX,UN}_{d,k} \tag{22}$$

The advanced exergy analysis is based on the ideal working with reversible processes. Therefore, if one changes one component with the real one, then the exergy destructions that occurred in the overall system is endogenous exergy destruction of the component since the others work under reversible conditions. According to advanced analysis, the improvement potential of the kth component is given by:

$$IP_k = \frac{\dot{E}x^{AV}_{d,k}}{\dot{E}x_{d,k}} \tag{23}$$

However, it would be more suitable to give this ratio in terms of y_k for the parametric studies in which the inlet or outlet conditions differ from each other. Besides, the whole component including the auxiliary equipment should be taken into account to determine the improvement potential. In this aim, it is best to identify the improvement potential in terms of the ratio of improved to improvable (y_k). The improved potential (IP^*) can then be identified as follows:

$$IP^* = \frac{y^{Real} - y^{i}}{y^{Real} - y^{Ideal}} \tag{24}$$

where y^{Ideal} and y^{Real} are the exergy destruction ratios of the ideal case and real case, respectively. y^{i} is avoidable exergy destruction rate for the handled case. Improved potential (IP^*) can be used for the comparison of the cases which are parametrically formed during the analysis. The real and ideal conditions should be identified first to perform the advanced exergy analysis. In this regard, these conditions are determined as given in Table 7.

According to Table 7, the different unavoidable cases in the number of six were determined to perform the improvement potential of the boiler. In Case I to III, the air preheating system (HE-I) was just taken into account. In this aim, the other parameters were saved. In Case IV, the exchanger group of the boiler, including superheater, reheater, and economizer, was handled together with the adapted dewatering system including HE-II/EH and dryer. In Case V, a different condition of Case IV, in which the boiler heat exchanger efficiencies were developed with the less energetic dewatering system, was handled. In Case VI, the effectiveness of Case V was saved to investigate the effect of boiler self-heat exchangers. Since all the parameters affect each other, the available maximum effectiveness was determined and analysed for Case IV and V.

Table 6
Energy and exergy balance equations of the components.

Component	Energy Balance	Exergy Balance
B	$\dot{E}_f + \dot{Q} + \dot{m}_1 h_1 + \dot{m}_3 h_3 - \dot{m}_2 h_2 - \dot{m}_4 h_4 = 0$	$\dot{E}x_{f,i} - \dot{E}x_{f,o} + \dot{E}x^{Q} + \dot{m}_1 \psi_1 + \dot{m}_3 \psi_3 - \dot{m}_2 h_2 - \dot{m}_4 h_4 = \dot{E}x_d$
HE-I	$\dot{Q} + \dot{W}_{fan} + \dot{m}_5 h_5 + \dot{m}_{14} h_{14} - \dot{m}_6 h_6 - \dot{m}_{15} h_{15} = 0$	$\dot{E}x^{Q} + \dot{m}_5 \psi_5 + \dot{m}_{14} \psi_{14} - \dot{m}_6 \psi_6 - \dot{m}_{15} \psi_{15} = \dot{E}x_d$
HE-II/EH*	$\dot{Q} - (\dot{W}_{fan} + \dot{W}_{EH}) + \dot{m}_7 h_7 + \dot{m}_{15} h_{15} - \dot{m}_8 h_8 - \dot{m}_{16} h_{16} = 0$	$\dot{E}x^{Q} + \dot{E}x^{W} + \dot{m}_7 \psi_7 + \dot{m}_{15} \psi_{15} - \dot{m}_8 \psi_8 - \dot{m}_{16} \psi_{16} = \dot{E}x_d$
Dryer	$\dot{Q} + \dot{m}_9 h_9 + \dot{m}_{11} h_{11} - \dot{m}_{10} h_{10} - \dot{m}_{12} h_{12} = 0$	$\dot{E}x^{Q} + \dot{m}_9 \psi_9 + \dot{m}_{11} \psi_{11} - \dot{m}_{10} \psi_{10} - \dot{m}_{12} \psi_{12} = \dot{E}x_d$

Table 7
Parameters of the real, ideal, and unavoidable conditions.

Component	Real (Measured) Case	Ideal Case	Unavoidable Case					
			Case I	Case II	Case III	Case IV	Case V	Case VI
B	η= 0.79*	η= 1.00	η= 0.79*	η= 0.79*	η= 0.79*	η= 0.90*	η= 0.95*	η= 0.85*
HE-I	η= 0.49	η= 1.00 ΔP = 0	η= 0.60 ΔP = 1%	η= 0.65 ΔP = 1%	η= 0.70 ΔP = 1%	η= 0.82 ΔP = 1%	η= 0.70 ΔP = 1%	η= 0.70 ΔP = 1%
HE-II/EH	–	–	–	–	–	$\eta_{HE\text{-}II}$= 0.82 η_{EH}= 0.99 ΔP = 2%	$\eta_{HE\text{-}II}$= 0.70 η_{EH}= 0.99 ΔP = 2%	$\eta_{HE\text{-}II}$= 0.70 η_{EH}= 0.99 ΔP = 2%
Dryer	–	–	–	–	–	η= 0.90 ΔP = 2%	η= 0.90 ΔP = 2%	η= 0.90 ΔP = 2%

* Effectiveness of boiler heat exchangers including superheater, reheater, and economizer.

Table 8
The real and ideal combustion conditions for the boiler.

Material	Compound	Unit	Value	
			Real condition	Ideal condition
Lignite (kmole/s)	C	kmole/s	0.011381	0.0166142
	S		0.000170	0.0002483
	N		0.000012	0.0000176
	O		0.001271	0.0018551
	H		0.014299	0.0208743
	$H_2O_{(fluid)}$		0.017499	–
Air (kmole/s)	N_2	kmole/s	0.110253	0.095671
	O_2	kmole/s	0.029323	0.025445
	x	–	0.017454	0.025444
Flue Gas (kmole/s)	CO_2	kmole/s	0.010875	0.016614
	CO		0.000505	–
	SO_2		0.000170	0.000248
	NO_2		0.000024	–
	N_2		0.110241	0.095689
	O_2		0.012120	–
	$H_2O_{(gaseous)}$		0.031798	0.020874

For the combustion process, the real condition is based on the measured values. The ideal conditions were determined considering the best attainable situation in theory. The combustion parameters for the real and ideal conditions are given in Table 8.

In the study, the unavoidable conditions were also parametrically handled. So, it was enabled to observe the degree of rehabilitation of the system. In this aim, the dewatered moisture ratio (*DMR*) and the effectiveness of the heat exchangers (η) were determined as the main parameters. In this regard, three main conditions were determined according to λ taken as 1.68 (which is the current value) and determined according to the available best λ *value*. According to the best of the authors' knowledge, the λ changes between 1.25 and 1.5 for effective combustion in the pulverized coal-fired boiler [8]. The most important factors are the pulverized coal size and water content that forms a slurry media that makes harder the incorporation of fuel and air. So, λ was selected as 1.30 for available effective combustion. The combustion parameters for the unavoidable cases are given in Table 9.

Table 10
The conventional exergy analysis results of the combustion process for ideal case, real case, and Case I to III.

Parameter	Unit	Ideal	Real	Case I	Case II	Case III
T_{cc}	(°C)	2392.8	1340.7	1378.7	1394.0	1409.6
$T_{lignite}$	(°C)	25.0	25.0	25.0	25.0	25.0
$\dot{m}$	(kg/s)	34.9	85.3	82.3	81.1	80.0
$\dot{Q}_i$	(kJ/kg)	–	4131.4	3906.2	3804.0	3700.3
$\dot{Q}_o$	(kJ/kg)	10,904.0	9777.2	9758.7	9740.3	9721.7
$\dot{E}x_i$	(kJ/kg)	–	3368.1	3201.2	3123.8	3044.7
$\dot{E}x_o$	(kJ/kg)	9684.6	7970.9	7997.3	7998.4	7999.2
$\dot{Q}_f$	(kJ/kg)	10,904.0	5645.9	5852.4	5936.3	6021.3
$\dot{E}x_f$	(kJ/kg)	9291.9	2648.7	2830.6	2901.8	2974.2
$\dot{E}x_d$	(kJ/kg)	392.7	1954.2	1965.5	1972.9	1980.3

3. Results and discussions

In the study, the combustion process was first analysed according to performed cases. Later, the conventional exergy analysis was conducted and the advanced exergy analysis was performed finally.

Table 9
The unavoidable combustion conditions (λ=1.30).

Material	Compound	*DMR* (%)			
		0	20	40	60
Lignite (kmole/s)	C	0.0113810	0.0121462	0.0130217	0.0140332
	S	0.0001701	0.0001815	0.0001946	0.0002097
	N	0.0000120	0.0000128	0.0000138	0.0000148
	O	0.0012708	0.0013562	0.0014540	0.0015669
	H	0.0142992	0.0152606	0.0163606	0.0176314
	$H_2O_{(fluid)}$	0.0174991	0.0149405	0.0120130	0.0086308
Air (kmole/s)	N_2	0.0852561	0.0909881	0.0975463	0.1051234
	O_2	0.0226745	0.0241990	0.0259432	0.0279584
	x	0.0174419	0.0186146	0.0199563	0.0215064
Flue Gas (kmole/s)	CO_2	0.0113810	0.0121462	0.0130217	0.0140332
	CO	–	–	–	–
	SO_2	0.0001701	0.0001815	0.0001946	0.0002097
	NO_2	0.0000120	0.0000128	0.0000138	0.0000148
	N_2	0.0852561	0.0909881	0.0975463	0.1051234
	O_2	0.0052300	0.0055900	0.0059800	0.0064500
	$H_2O_{(gaseous)}$	0.0317983	0.0302011	0.0283736	0.0262622

Table 11
The conventional exergy analysis results of the combustion process for Case IV and Case V.

Parameter		*DMR* (%)											
		Case IV				Case V				Case VI			
		0	20	40	60	0	20	40	60	0	20	40	60
T_{cc}	(°C)	1618.6	1700.7	1784.2	1874.9	1555.8	1633.1	1711.4	1796.2	1624.1	1707.6	1792.7	1885.3
$T_{lignite}$	(°C)	25.0	39.2	39.2	39.2	25.0	39.2	39.2	39.2	25.0	39.2	39.2	39.2
$\dot{m}$	(kg/s)	63.5	57.8	52.5	47.5	60.4	55.0	50.0	45.3	70.3	63.9	58.1	52.5
$\dot{Q}_i$	(kJ/kg)	4123.0	3291.3	2365.8	1286.8	4469.9	3677.5	2797.3	1772.3	4092.5	3251.7	2315.4	1222.6
$\dot{Q}_o$	(kJ/kg)	10,781.0	10,608.0	10,412.1	10,184.4	11,104.9	10,964.5	10,804.8	10,619.8	10,462.8	10,256.3	10,023.0	9751.5
$\dot{E}x_i$	(kJ/kg)	3473.2	2794.2	2022.9	1108.2	3741.2	3102.3	2377.0	1517.0	3449.3	2762.7	1981.3	1053.7
$\dot{E}x_o$	(kJ/kg)	9081.9	9005.7	8903.1	8770.8	9294.6	9249.5	9181.5	9089.7	8818.5	8712.5	8576.4	8404.5
$\dot{Q}_f$	(kJ/kg)	6658.0	7316.7	8046.3	8897.6	6635.0	7287.0	8007.6	8847.5	6370.3	7004.7	7707.6	8528.9
$\dot{E}x_f$	(kJ/kg)	4086.4	5435.6	6213.4	7134.6	4266.7	5434.0	6195.1	7095.6	3773.5	5110.3	5856.7	6739.7
$\dot{E}x_d$	(kJ/kg)	1522.2	775.9	666.8	528.1	1286.7	713.2	609.4	477.1	1595.7	840.0	738.5	611.1

Table 12
Technical data of the handled system for real condition, ideal condition, and Case I to III.

State	Fluid	Real			Ideal			Case I			Case II			Case III		
		$\dot{m}$ (kg/s)	T (°C)	P (bar)	$\dot{m}$ (kg/s)	T (°C)	P (bar)	$\dot{m}$ (kg/s)	T (°C)	P (bar)	$\dot{m}$ (kg/s)	T (°C)	P (bar)	$\dot{m}$ (kg/s)	T (°C)	P (bar)
0	–	–	25.0	1.0	–	25.0	1.0	–	25.0	1.0	–	25.0	1.0	–	25.0	1.0
1	Water	131.9	220.0	157.3	131.9	220.0	157.3	131.9	220.0	157.3	131.9	220.0	157.3	131.9	220.0	157.3
2	Water	131.9	538.0	137.3	131.9	538.0	137.3	131.9	538.0	137.3	131.9	538.0	137.3	131.9	538.0	137.3
3	Water	120.5	349.0	34.3	120.5	349.0	34.3	120.5	349.0	34.3	120.5	349.0	34.3	120.5	349.0	34.3
4	Water	120.5	538.0	33.8	120.5	538.0	33.8	120.5	538.0	33.8	120.5	538.0	33.8	120.5	538.0	33.8
5	Air	343.2	25.0	1.0	235.2	25.0	1.0	331.1	25.0	1.0	326.4	25.0	1.0	321.8	25.0	1.0
6	Air	343.2	236.7	1.0	235.2	220.0	1.0	331.1	290.1	1.0	326.4	314.3	1.0	321.8	338.9	1.0
7	Air	–	–	–	–	–	–	–	–	–	–	–	–	–	–	–
8	Air	–	–	–	–	–	–	–	–	–	–	–	–	–	–	–
9	Air	–	–	–	–	–	–	–	–	–	–	–	–	–	–	–
10	Air	–	–	–	–	–	–	–	–	–	–	–	–	–	–	–
11	Lignite	85.3	25.0	–	34.9	25.0	–	82.3	25.0	1.0	81.1	25.0	–	80.0	25.0	–
12	Lignite	388.1	458.7	–	132.7	220.0	–	374.5	466.8	1.0	369.3	470.1	–	364.0	473.4	–
13	Flue gases	388.1	291.1	–	132.7	55.1	–	374.5	255.3	1.0	369.3	238.6	–	364.0	221.6	–
14	Flue gases	–	–	–	–	–	–	–	–	–	–	–	–	–	–	–

Table 13
Technical data of the handled system for Case IV and Case V.

State	Fluid	Case IV			Case V			Case VI		
		$\dot{m}$ (kg/s)	T (°C)	P (bar)	$\dot{m}$ (kg/s)	T (°C)	P (bar)	$\dot{m}$ (kg/s)	T (°C)	P (bar)
0	–	–	25.0	1.0	–	25.0	1.0	–	25.0	1.0
1	Water	131.9	220.0	157.3	131.9	220.0	157.3	131.9	220.0	157.3
2	Water	131.9	538.0	137.3	131.9	538.0	137.3	131.9	538.0	137.3
3	Water	120.5	349.0	34.3	120.5	349.0	34.3	120.5	349.0	34.3
4	Water	120.5	538.0	33.8	120.5	538.0	33.8	120.5	538.0	33.8
5	Air	192.0	25.0	–	182.6	25.0	–	212.3	25.0	–
6	Air	192.0	306.3	–	182.6	211.0	–	212.3	224.0	–
7	Air	393.8	25.0	–	374.6	25.0	–	435.5	25.0	–
8	Air	393.8	100.0	–	374.6	100.0	–	435.5	100.0	–
9	Air	397.4	78.0	–	378.0	78.0	–	439.5	78.0	–
10	Air	61.7	25.0	–	58.7	25.0	–	68.2	25.0	–
11	Lignite	57.8	39.2	–	55.0	39.2	–	63.9	39.2	–
12	Lignite	220.6	368.1	–	210.7	290.7	–	516.1	443.1	–
13	Flue gases	220.6	158.1	–	210.7	167.0	–	516.1	224.0	–
14	Flue gases	220.6	131.9	–	210.7	133.6	–	516.1	191.5	–

3.1. Results of the combustion process

In the real case, ideal case, and Case I to III, the situation of single air preheating was handled and the results are given in Table 10.

According to Table 10, although exergy destruction increases the energy and exergy values of the fuel increase by improving the air preheater (HE-I) effectiveness as expected. The increased rate of exergy destruction is slight where the exergy of fuel has a relatively sharp increase. Therefore, the efficiency of the boiler would increase definitively. In Case IV to VI, the situations of both air preheating and dewatering processes were handled. The results of these cases are given in Table 11.

According to Table 11, as in the single preheating cases, the exergy destruction increases slightly where the energy and exergy of the fuel increase sharply. However, the exergy increase rate has a more distinct increase caused by the decrease of excess air and the removal of the water content of the fuel.

Table 14
Conventional exergy analysis results for real, ideal cases and Case I to III.

Component	Value (kW)							Value (%)		
	$\dot{E}_i$	$\dot{E}_o$	$\dot{Q}$	$\dot{W}$	$\dot{E}x_i$	$\dot{E}x_o$	$\dot{E}x_d$	ε	y	y^*
Real										
B	980,174.9	879,017.9	−101,157.0	–	553,808.8	374,748.2	345,788.4	37.56	55.99	69.78
HE-I	1691,143.1	1357,953.4	−333,189.6	–	360,171.9	210,430.3	149,741.7	58.42	24.25	30.22
HE-II	–	–	–	–	–	–	–	–	–	–
Dryer	–	–	–	–	–	–	–	–	–	–
Overall system					*617,535.2*	*396,244.6*	*495,530.1*	*19.76*	*80.24*	*100.00*
Ideal										
B	879,017.9	879,017.9	–	–	499,084.2	361,482.7	140,157.1	71.92	27.70	99.53
HE-I	35,606.1	30,757.5	−4848.6	–	2437.5	1781.8	655.6	73.10	0.13	0.47
HE-II	–	–	–	–	–	–	–	–	–	–
Dryer	–	–	–	–	–	–	–	–	–	–
Overall system					*506,000.27*	*361,547.39*	*140,812.70*	*72.17*	*27.83*	*100.00*
Case I										
B	980,174.9	879,017.9	−101,157.0	–	555,856.5	374,748.2	342,886.9	38.31	54.09	72.45
HE-I	1652,230.1	1249,286.2	−402,943.9	–	358,425.0	228,013.8	130,411.2	63.62	20.57	27.55
HE-II	–	–	–	–	–	–	–	–	–	–
Dryer	–	–	–	–	–	–	–	–	–	–
Overall system					*633,879.8*	*387,604.2*	*473,298.0*	*25.33*	*74.67*	*100.00*
Case II										
B	980,174.9	879,017.9	−101,157.0	–	556,656.0	374,748.2	341,995.8	38.56	53.36	73.34
HE-I	1636,854.2	1203,774.1	−433,080.1	–	357,682.2	233,390.5	124,291.8	65.25	19.39	26.66
HE-II	–	–	–	–	–	–	–	–	–	–
Dryer	–	–	–	–	–	–	–	–	–	–
Overall system					*640,884.3*	*384,064.5*	*466,287.5*	*27.24*	*72.76*	*100.00*
Case III										
B	980,174.9	879,017.9	−101,157.0	–	557,452.0	374,748.2	341,123.7	38.81	52.66	73.98
HE-I	1621,692.3	1159,203.6	−462,488.7	–	356,965.3	237,013.6	119,951.7	66.40	18.52	26.02
HE-II	–	–	–	–	–	–	–	–	–	–
Dryer	–	–	–	–	–	–	–	–	–	–
Overall system					*647,830.1*	*380,733.9*	*461,075.4*	*28.83*	*71.17*	*100.00*

Table 15
Conventional exergy analysis results for Case IV, V, and VI.

Component	Value (kW)							Value (%)		
	$\dot{E}_i$	$\dot{E}_o$	$\dot{Q}$	$\dot{W}$	$\dot{E}x_i$	$\dot{E}x_o$	$\dot{E}x_d$	ε	y	y^*
Case IV (λ=1.30, η_B = 0.90, $\eta_{HE\text{-}I}$ = $\eta_{HE\text{-}II}$ = 0.82, *DMR*=20%)										
B	921,300.5	879,017.9	−42,282.6	–	520,057.0	367,027.5	197,870.8	61.95	37.09	79.16
HE-I	716,480.4	537,055.4	−179,424.9	–	117,914.6	78,097.4	39,817.2	66.23	7.46	15.93
HE-II	539,794.0	547,225.6	7431.6	7791.9	30,218.9	18,460.0	11,758.9	61.09	2.20	4.70
Dryer	185,037.6	174,628.8	−10,408.8	28.7	4092.9	3576.8	516.1	87.39	0.10	0.21
Overall system					*533,419.8*	*378,200.6*	*249,963.0*	*53.14*	*46.86*	*100.00*
Case V (λ=1.30, η_B = 0.95, $\eta_{HE\text{-}I}$ = $\eta_{HE\text{-}II}$ = 0.70, *DMR*=20%)										
B	899,046.5	879,017.9	−20,028.6	–	499,019.8	364,109.2	174,117.8	65.11	34.45	83.55
HE-I	595,081.2	500,244.5	−94,836.7	–	72,543.7	44,745.0	27,798.7	61.68	5.50	13.34
HE-II	522,704.3	522,311.3	−392.9	–	24,002.1	18,002.1	6000.0	75.00	1.19	2.88
Dryer	176,014.4	166,113.2	−9901.2	27.3	3893.3	3402.4	490.9	87.39	0.10	0.24
Overall system					*505,438.2*	*377,816.6*	*208,407.3*	*58.77*	*41.23*	*100.00*
Case VI (λ=1.30, η_B = 0.85, $\eta_{HE\text{-}I}$ = $\eta_{HE\text{-}II}$ = 0.70, *DMR*=20%)										
B	946,172.5	879,017.9	−67,154.6	–	541,408.4	370,289.2	224,804.9	58.48	39.21	75.66
HE-I	893,253.5	677,057.9	−216,195.6	–	181,611.2	119,827.9	61,783.3	65.98	10.77	20.79
HE-II	677,292.5	676,829.2	−463.3	–	50,986.9	41,005.6	9981.3	80.42	1.74	3.36
Dryer	204,650.4	193,138.3	−11,512.0	31.8	4526.7	3955.9	570.8	87.39	0.10	0.19
Overall system					*573,396.4*	*374,840.0*	*297,140.3*	*48.18*	*51.82*	*100.00*

3.2. Results of conventional exergy analysis

Exergy analyses were conducted considering different parameters. According to performed cases, the effectiveness of heat exchangers, excess air ratio, and removed water content ratio was taken as parameters to improve the boiler efficiency. The inlet and outlet conditions of the water and steam line were kept constant to observe solely the boiler improvement. Pressure drops were taken as 2% of inlet conditions that means 0.02 bar for the parasitic losses in heat exchangers and piping systems. Since the current system is the worst one and is already met by generated power from the turbine, the pressure drops, and the required power for the circulation of air was not included in the analysis. For the dewatering subsystem, the outlet relative moisture ratio was adjusted as 17% with the consideration of worst inlet conditions as 100% for a rainy weather condition. The values of the states for the handled system are given in Tables 12 and 13 (just for *DMR*=20%).

The exergy analysis was conducted according to the data given in Tables 12 and 13. The obtained results for ideal case, real case, and cases I to III are given in Table 14. According to Table 14, the maximum efficiency (ideal case) was determined as 71.92 and 72.17% for the boiler and overall system, respectively. These values are orderly

37.56 and 19.76% for the real case. As seen from these results, the overall efficiency is relatively lower in comparison to boiler efficiency owing to the lower efficiency of HE-I. In this aim, the cases including the improved HE-I were conducted. Depending on the increasing efficiency of HE-I, the exergy efficiency values of the boiler increase slightly where the exergy efficiency values of overall systems increase relatively sharply. This result can be interpreted as it has a low impact on the combustion process. However, this impact on the overall system is relatively higher since the waste heat is evaluated. The obtained results for Case IV, V, and VI with *DMR* = 20% are given in Table 15.

In Table 15, the effectiveness of HE-I and HE-II were determined to obtain the available highest outlet conditions. In this regard, it is possible to increase the efficiency value by up to 58.77%. As seen from the results of the analysis, although the effectiveness of HE-I and HE-II decreases the exergy efficiency values of this auxiliary equipment and overall system increase. This finding shows that the effectiveness of the self-heat exchanger group of the boiler is more important than the auxiliary ones. This exchanger group also would affect the other state points of the whole plant positively. For the other parameters, the obtained exergy efficiency values are given in Fig. 2.

As seen in Fig. 2, the efficiency increase with the decrease of excess air as expected. According to the best of knowledge, the efficiency should continuously increase with the increase of removed water. However, in this study, the efficiency increases with the increase of *DMR* up to a certain point of 20%. After this point, a decrease in this value is observed. This means the energy value of the flue gases has a self-ability to remove the water content of fuel or the required electrical energy is relatively lower. After this point, the required electrical energy increases sharply and makes the efficiency decrease. The variation of required electrical power is given in Fig. 3.

For the best condition, the exergy efficiency of the overall system was determined as 53.14, 58.77, and 48.46% for Case IV Case V, and Case VI, respectively.

3.3. Results of advanced exergy analysis

Advanced exergy analysis was conducted to perform the improvement ability on the efficiency of the boiler system. In this aim, the unavoidable exergy destruction values were calculated. The obtained results are given in Figs. 4 and 5 for the single boiler and air preheater, respectively.

According to Fig. 4, the unavoidable exergy destruction of the boiler (existing total exergy destruction) was calculated as 345,788.4 kW for the real case where it was calculated as 140,157.1 kW for the ideal case. Depending on the formed unavoidable cases, this destruction decreases down to 161,452.4 kW. The main reason for this decrease is the increase in the efficiency of the self-heat exchangers of the boiler. Besides, the dewatering process also positively affects the combustion process.

According to Fig. 5, the unavoidable (or existing) exergy destruction of the real case was calculated as 149,741.7 kW where that of the ideal case was calculated as 655.6 kW. This destruction increases by the increase of *DMR* for Case IV and Case VI. For Case V, it is almost constant with a relatively lower increase. However, these increases are relatively lower ranging between 0.95%–1.69% for Case VI, and 1.28%–1.95% for Case VI. For Case V, this rate ranges between

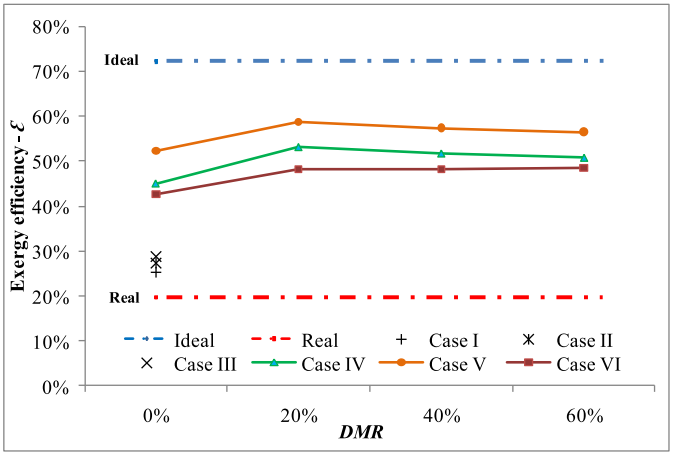

Fig. 2. Exergy efficiency variation versus *DMR*.

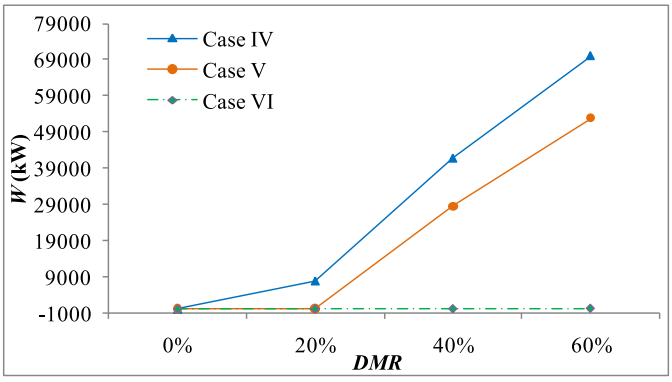

Fig. 3. Required electrical energy for the dewatering process.

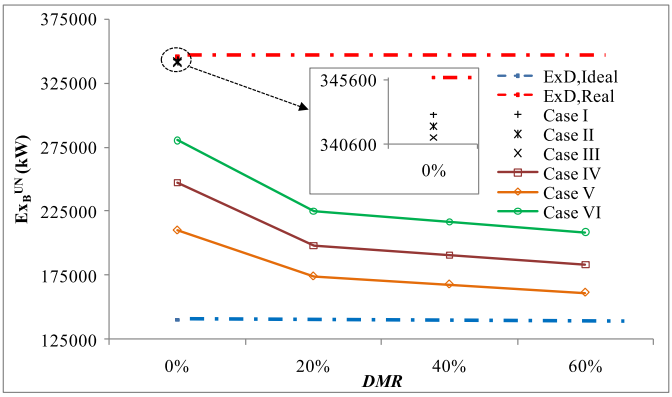

Fig. 4. Unavoidable exergy destruction change for the single boiler.

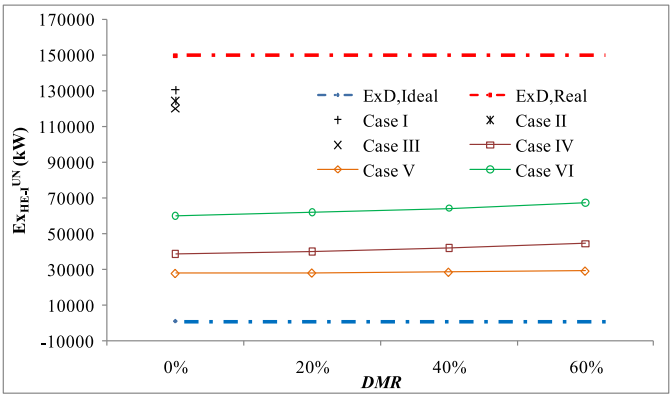

Fig. 5. Unavoidable exergy destruction change for single HE-I.

0.16%–0.40%. The main reason for this lower impact is the increase in the efficiency of the HE-I that makes a negative effect on HE-II depending on the decrease of quality of waste heat in the flue gases.

As seen from the handled cases, the boiler system should be evaluated together with the auxiliary air preheating and dewatering subsystems as a whole since some do not include both processes. So, the unavoidable exergy destruction of the whole system, named as combustion system (*CS*) in the rest of the text, is given in Fig. 6.

According to Fig. 6, the unavoidable exergy destruction values of *CS* change between 208,407.3 kW and 473,298.1 for the performed unavoidable cases. The exergy destruction value of the real system is 495,530.1 kW where that of the ideal case is 140,812.7 kW. For Case I to III, this value decrease by the increase in the effectiveness of HE-I since the conditions of preheating air is developed. However, this decrease, ranging between 4.49%–6.95%, is relatively lower in comparison to other cases ranging between 31.35%–57.94%. For Case IV and Case V, unavoidable exergy destruction decreases by the increase of *DMR* up to 20% of removed water. Later this point, this value starts to increase again. The main factor of this event lies in the quality and quantity of the flue gas energy. With the increase of efficiency of the self-heat exchanger of the boiler, the energy quality of flue gas decrease since most of this energy is used for the heating purpose of the steam. After 20% of *DMR*, the self-energy of flue gases is not sufficient, so extra energy is required supplied from the external electrical heat source. For Case VI, unavoidable exergy destruction also decreases by the increase of *DMR* up to 20% of removed water. After this breaking point, it is almost constant since the recuperation of combustion air and dewatering process effects are in the same measure of the external electrical demand for the dewatering process.

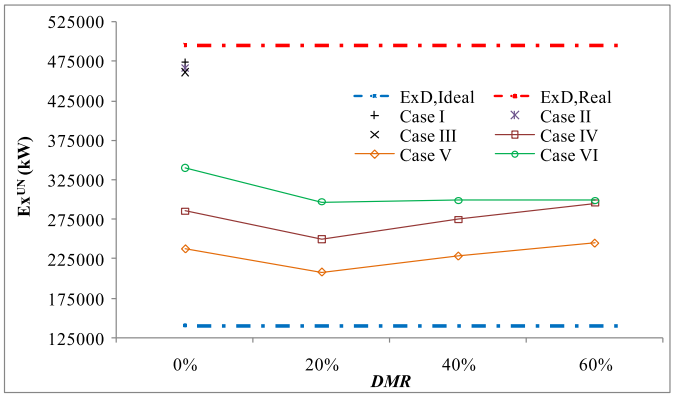

Fig. 6. Unavoidable exergy destruction change for *CS*.

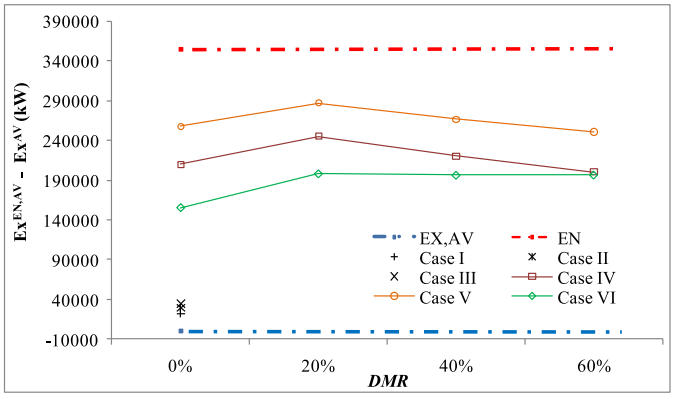

Fig. 7. Avoidable exergy destruction change for *CS*.

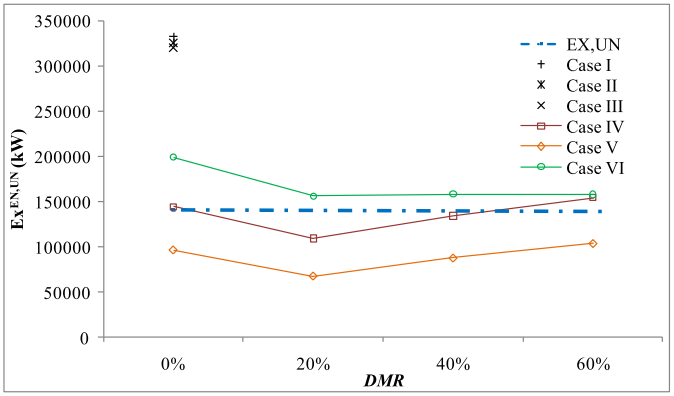

Fig. 8. Endogenous unavoidable exergy destruction change for *CS*.

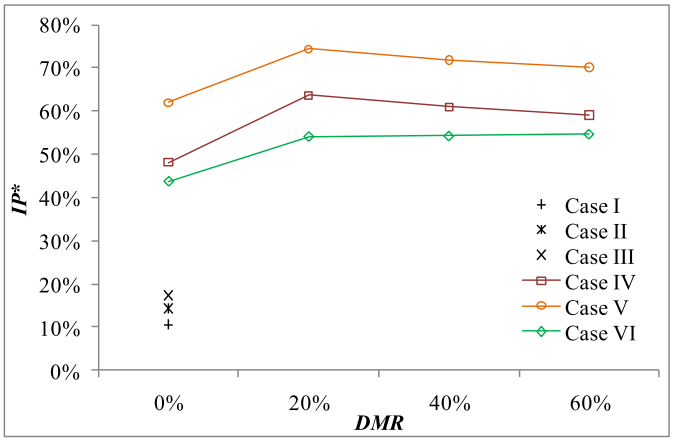

Fig. 9. Improved potential variation of *CS*.

The same trend is also acceptable for the avoidable part of exergy destruction as given in Fig. 7.

According to Fig. 7, the avoidable exergy destruction value changes between 22,232.0 kW and 287.122.8 kW for the performed cases. The total endogenous exergy destruction was calculated as 354,717.4 kW. The exogenous avoidable exergy destruction is zero as expected since the single component of the power plant (*CS*) was investigated where the outlet conditions were kept constant to observe the changes. So, the avoidable and endogenous avoidable parts of exergy destruction equal to each other.

Because of the same reason, the exogenous unavoidable part is also constant with a value of 140,812.7 kW. The variation of the unavoidable part is given in Fig. 8.

According to Fig. 8, the endogenous unavoidable exergy destruction trend is the same as the unavoidable one. In Case VI, the decrease is continuous after breaking point at 20% of DMR in contrast to Case IV and Case V. Even so, the endogenous unavoidable exergy destruction of Case IV and Case V is less than that of Case VI. This result once again shows that the self-heat exchangers such as economizer, reheater, and superheater need to be improved primarily. The change in the improved potential of *CS* is given in Fig. 9.

According to Fig. 9, the maximum improved potential is obtained with 74.4% for Case V at 20% of *DMR*. This means it is available to catch 74.4 percent of the maximum avoidable conditions (100%) of the ideal case. For all cases having the dewatering process, 20% of *DMR* is the critical point. After this point, the improved potential starts to decrease for Case IV and V. For Case VI, it continues to increase slightly. The main source of this different behaviour from those of Case IV and V is the lower effectiveness of self-heat

exchangers of the boiler. So, the flue gas at the outlet of the boiler has more qualitative energy with its higher temperature. Moreover, the potential is still lower than that of Case IV and Case V depending on the self-heat changers' effectiveness once more. The variation of the effectiveness of HE-I and HE-II directly affects the incline of the potential curves as seen in the figure. Moreover, the higher effectiveness results in a higher potential change. The measure of the effect of HE-I and HE-II on the improved potential of *CR* is about 1.68 points per 1% increase in the effectiveness. As seen in the figure, the best avoidable conditions obtained for 20% of *DMR*. The measure of the effect of removed water is about 0.62 points per removed water of 1%. The measure of the effect of self-heat exchangers on the improved potential of *CR* is about 2.8 points per 1% increase in the effectiveness.

4. Conclusion

In this study, parametric advanced exergy analysis was conducted to perform the improvement ability of a boiler (combustion) system of a pulverized coal-fired power plant. In this aim, different unavoidable cases were formed in which different parameters were evaluated. In these cases, the air preheating system was first handled and the rehabilitated system was investigated from the viewpoint of different technically possible effectiveness values. Then, the dewatering system and air preheating system were coupled to the boiler system and analysed for different removed moisture ratios from the coal. All these cases were finally evaluated under the definition of improved potential. The following main findings were concluded:

- A new attainable ideal case and technically available unavoidable case were identified. In this way, the highest improved potential was determined as 74.4%.
- The self (internal) heat exchangers of the boiler are found the most suitable parts to be rehabilitated. Its effect was determined as 2.8 points per 1% effectiveness increase.
- The second most effective parts were determined as HE-I and HE-II (external heat exchangers) with 1.68 points per 1% effectiveness increase.
- The most appropriate ratio of removed moisture content was determined as 20% for the handled lignite with high moisture content. The effect of removed moisture was determined as 0.62 points per 1% *DMR*.
- All these rehabilitations are practicable and bring some different latent benefits depending on the decrease in fuel consumption. Moreover, it is available to save 29.54% of consumed coal in comparison to the real (measured) case. It means a reduction of 0.22 g per generated power. This also means a decrease in emissions at the same rate.

Declaration of Competing Interest

The authors declare that they have no known competing financial interests or personal relationships that could have appeared to influence the work reported in this paper.

References

[1] ETKB (Republic of Turkey Ministry of Energy and Natural Resources). Data for electricity generation in Turkey. Available from https://www.enerji.gov.tr/en-US/Pages/Electricity Last Access: April 2020.

[2] Gao J, Zhang Q, Wang X, Song D, Liu W, Liu W. Exergy and exergoeconomic analyses with modeling for CO_2 allocation of coal-fired CHP plants. Energy 2018;152:562–75.

[3] Adibhatla S, Kaushik SC. Energy and exergy analysis of a supercritical thermal power plant at various load conditions under constant and pure sliding pressure operation. Appl Therm Eng 2014;73:51–65.

[4] Yang Y, Wang L, Dong C, Xu G, Morosuk T, Tsatsaronis G. Comprehensive exergy-based evaluation and parametric study of a coal-fired ultra-supercritical power plant. Appl Energy 2013;112:1087–99.

[5] Hong X, Chen J, Lyu H, Sheng D, Li W, Li H. Advanced exergoenvironmental evaluation for a coal-fired power plant of near-zero air pollutant emission. Appl Therm Eng 2018;128:1139–50.

[6] Regulagadda P, Dincer I, Naterer GF. Exergy analysis of a thermal power plant with measured boiler and turbine losses. Appl Therm Eng 2010;30:970–6.

[7] Oktay Z. Investigation of coal-fired power plants in Turkey and a case study: can plant. Appl Therm Eng 2009;29:550–7.

[8] Arslan O, Senturk MA. Enhanced exergetic evaluation of regenerative and recuperative coal-fired power plant. Int J Exergy 2020 in press.

[9] Chauhan SS, Khanam S. Enhancement of efficiency for steam cycle of thermal power plants using process integration. Energy 2019;173:364–73.

[10] Li Y, Liu L. Exergy Analysis of 300MW Coal-Fired Power Plant. Energy Procedia 2012;17:926–32.

[11] Rocha DHD, Silva RJ. Exergoenvironmental analysis of an ultra-supercritical coal-fired power plant. J Clean Prod 2019;231:671–82.

[12] Shi Y, Liu Q, Shao Y, Zhong W. Energy and exergy analysis of oxy-fuel combustion based on circulating fluidized bed power plant firing coal, lignite and biomass. Fuel 2020;269:117424.

[13] Song W, Quyang Z, Wang M, Li S, Liu J, Yu Q, Liu W, Zhu S. The combustion and NO_x emission characteristics of the ultra-low volatile fuel using the novel pulverized coal self-sustained preheating combustion technology. Fuel 2020;271:117592.

[14] Chen H, Wu Y, Qi Z, Chen Q, Xu G, Yang Y. Improved combustion air preheating design using multiple heat sources incorporating bypass flue in large-scale coal-fired power nit. Energy 2019;169:527–41.

[15] Chen H, Qi Z, Dai L, Li B, Hu G, Yang Y. Performance evaluation of a new conceptual combustion air preheating system in a 1000 MW coal-fueled power plant. Energy 2020;193:16739.

[16] Yan M, Zhang L, Shi Y, l Zhang, Li Y, Ma C. A novel boiler cold-end optimization system based on bypass flue in coal-fired power plants, 152. Heat recovery from wet flue gas. Energy; 2018. p. 84–94.

[17] Ma Y, Wang A, Lyu J, Wang Z. Techno-economic evaluation of the novel hot air recirculation process for exhaust heat recovery from a 600 MW hard-coal-fired boiler. Energy 2020;200:117558.

[18] Liu M, Yan J, Wang J, Chong D, Liu J. Thermodynamic analysis on a pre-dried lignite-fired power system: comparison on energy supply systems for dryer. Energy Procedia 2014;61:1924–7.

[19] Ge L, Zhang Y, Xu C, Wang Z, Zhou J, Cen K. Influence of the hydrothermal dewatering on the combustion characteristics of Chinese low-rank coals. Appl Therm Eng 2015;90:174–81.

[20] Wang WC. Laboratory investigation of drying process of Illinois coals. Powder Technol 2012;225:72–85.

[21] Liu M, Yan J, Chong D, Liu J, Wang J. Thermodynamic analysis of pre-drying methods for pre-dried lignite-fired power plant. Energy 2013;49:107–18.

[22] Kakaras E, Ahladas P, Syrmopoulos S. Computer simulation studies for the integration of an external dryer into a Greek lignite-fired power plant. Fuel 2002;81:583–93.

[23] Agraniotis M, Koumanakos A, Doukelis A, Karellas S, Kakaras E. Investigation of technical and economic aspects of pre-dried lignite utilisation in a modern lignite power plant towards zero CO_2 emissions. Energy 2012;45:134–41.

[24] Liu M, Jan J, Bai B, Chong D, Guo X, Xiao F. Theoretical study and case analysis for a predried lignite-fired power system. Drying Technol 2011;29:1219–29.

[25] Xu C, Xu G, Zhao S, Zhou L, Yang Y, Zhang D. An improved configuration of lignite pre-drying using a supplementary steam cycle in a lignite fired supercritical power plant. Appl Energy 2015;160:882–91.

[26] Atsonios K, Violidakis I, Agraniotis M, Grammelis P, Nikolopoulos N, Kakaras E. Thermodynamic analysis and comparison of retrofitting pre-drying concepts at existing lignite power plants. Appl Therm Eng 2015;74:165–73.

[27] Lieberman N. Effect of Combustion Air Preheat on a Fired Heater. Effect of Combustion Air Preheat on a Fired Heater. Understanding process equipment for operators and engineers, chapter:21. Elsevier; 2019.

[28] Allardice DJ, Clemow LM, Favas G, Jackson WR, Marshall M, Sakurovs R. The characterisation of different forms of water in low rank coals and some hydrothermally dried products. Fuel 2003;82:661–7.

[29] Binner E, Zhang L, Li CZ, Bhattacharya S. *In-situ* observation of the combustion of air-dried and wet Victorian brown coal. In: Proceedings of the combustion institute, 33; 2011. p. 1739–46.

[30] Wang S, Niu Y, Li T, Wang F, Hui S. Experimental and kinetic study on the transformation of coal nitrogen in the preheating stage of preheating-combustion coupling process. Fuel 2020;275:117924.

[31] Kruczek HP, Niedzwiecki L, Ostrycharczyka M, Czerep M, Plutecki Z. Potential and methods for increasing the flexibility and efficiency of the lignite-fired power unit, using integrated lignite drying. Energy 2019;181:1142–51.

[32] Rao Z, Zhao Y, Huang C, Duan C, He J. Recent developments in drying and dewatering for low rank coals. Prog Energy Combust Sci 2015;46:1–11.

[33] Han X, Liu M, Wang J, Yan J, Liu J, Xiao F. Simulation study on lignite-fired power system integrated with flue gas drying and waste heat recovery – Performances under variable power loads coupled with off-design parameters. Energy 2014;76:406–18.

[34] Han X, Liu M, Zhai M, Chong D, Yan J, Xiao F. Investigation on the off-design performances of flue gas pre-dried lignite-fired power system integrated with waste heat recovery at variable external working conditions. Energy 2015;90:1743–58.

[35] Han X, Liu M, Wu K, Chen W, Xiao F, Yan J. Exergy analysis of the flue gas predried lignite-fired power system based on the boiler with open pulverizing system. Energy 2016(106):285–300.
[36] Nikolopoulos N, Violidakis I, Karampinis E, Agraniotis M, Bergins C, Grammelis P, Kakaras E. Report on comparison among current industrial scale lignite drying technologies (A critical review of current technologies). Fuel 2015;155:86–114.
[37] Ucar M, Arslan O. Assessment of improvement potential of a condensed combi boiler via advanced exergy analysis. Thermal Sci Eng Progr 2021;23:100853.
[38] Li X, Song H, Wang Q, Meesri C, Wall T, Yu J. Experimental study on drying and moisture re-adsorption kinetics of an Indonesian low rank coal. J Environ Sci 2009(21):127–30.
[39] Acar MS, Saraydar M, Arslan O. Exergetical evaluation of lignite production process: SLI case study. J Polytechnic 2018;21:55–63.
[40] Arslan O. M.*Sc*. Thesis. Institute of Applied Sciences, Dumlupinar University; 2005.
[41] Bejan A, Tsatsaronis G, Moran M. Thermal design and optimization. New York: John Wiley & Sons Inc.; 1996.
[42] Arslan O, Ozgur MA, Yildizay HD, Kose R. Fuel effects on optimum insulation thickness: an exergetic approach. Energy Sources Part A Recov Utilizat Environ Effects 2010;32:128–47.
[43] Cengel YA, Boles MA. Thermodynamics: an engineering approach. New York: McGraw Hill Inc.; 1994.
[44] Kelly S, Tsatsaronis G, Morosuk T. Advanced exergetic analysis: approaches for splitting the exergy destruction into endogenous and exogenous parts. Energy 2009;34:384–91.
[45] Tsatsaronis G, Park MH. On the avoidable and unavoidable exergy destructions and investment costs in thermal systems. Energy Convers Manag 2002;43:1259–70.
[46] Morosuk T, Tsatsaronis G. Advanced exergetic evaluation of refrigeration machines using different working fluids. energy, 34; 2009. 2548-2458.